PHYSICAL REVIEW B VOLUME 57, NUMBER 10 1 MARCH 1998-II

# Evidence of quadrupolar transitions in the circular dichroism at the neodymium $L_2$ and $L_3$ edges

Jesús Chaboy
*Instituto de Ciencia de Materiales de Aragón and Departamento de Física de la Materia Condensada, CSIC-Universidad de Zaragoza, 50009 Zaragoza, Spain*

Fernando Bartolomé
*Laboratoire de Cristallographie, CNRS, BP166, 38042 Grenoble, France*

Luis M. García
*Instituto de Ciencia de Materiales de Aragón and Departamento de Física de la Materia Condensada, CSIC-Universidad de Zaragoza, 50009 Zaragoza, Spain*

Giannantonio Cibin
*I.N.F.N., Laboratori Nazionali di Frascati—C.P. 13, 00044 Frascati, Italy*

(Received 16 December 1997)

The temperature dependence of the x-ray magnetic circular dichroism (XMCD) at both the Nd $L_2$ and $L_3$ edges in $Nd_2Fe_{14}B$ has been studied to ascertain the multipolar nature of the features in the dichroic spectra below the absorption edges. As this compound exhibits a spin reorientation transition at low temperatures, XMCD reflects the modification of the angle between the photon wave vector and the magnetization direction as a function of temperature. The angular dependence of the features below both the $L_2$ and $L_3$ absorption edges is determined to correspond to that proposed for quadrupolar transitions. [S0163-1829(98)50610-8]

In the past few years, the advent of intense, tunable, polarized synchrotron radiation sources has stimulated worldwide interest in using x rays to address magnetic aspects in the electronic structure and magnetism of condensed matter. Special attention has been paid to x-ray magnetic circular dichroism (XMCD) in core-level photoabsorption because it has been revealed as a unique element-selective magnetic probe. To this respect, the derivation of the sum rules for the dichroic signal, showing the relationship of the XMCD to the local spin and orbital magnetic moments,[1] constitutes a critical success in the development of the field. The sum rules have been experimentally verified for the transition metal ($M$) $L_{2,3}$ and rare-earth ($R$) $M_{4,5}$ absorption edges,[2] i.e., for $M$-$3d$ and $R$-$4f$ magnetic moments. However, for $R$-$M$ intermetallic materials it is also desirable to obtain information on the $R$-$5d$ conduction electrons, that mediate the magnetic interaction between the transition-metal and rare-earth sublattices, i.e., the competition of itinerant and localized magnetism.

The magnetic characterization of these conduction electrons is not solved by using standard techniques, therefore the possibility of applying the XMCD sum rules to obtain information about these states is a stimulating challenge. Indeed, extensive series of experiments have been performed since the first observation of XMCD in the $L_{2,3}$ edges of rare-earth compounds.[3] However, their interpretation is a matter of debate because they do not follow simple rules, so that a complete understanding of the features present in the XMCD spectra is still needed. One of the main open questions regards the dipolar or quadrupolar origin of the features typically observed in the XMCD spectra recorded at the $L_{2,3}$ edges of rare earths. Whereas features above the absorption edge in these spectra have unambiguously been assigned to dipolar ($2p \rightarrow 5d$) transitions ($E1$), the origin of the prominent peaks below the edge is still uncertain. These features were ascribed to quadrupolar ($2p \rightarrow 4f$) transitions ($E2$).[4] Experimental verification of Carra's proposition was provided, at the Gd $L_3$ edge, by resonant inelastic x-ray scattering (RIXS),[5] and by the observation at the Dy $L_3$ XMCD of the angular dependence predicted for features associated with quadrupolar transitions.[6]

As pointed out by Lang *et al.*, identification of these quadrupolar features in the dichroic spectra is essential in correctly applying the sum rules because dipolar and quadrupolar transitions obey distinct sum rules. However, a disturbing point remaining is that a quadrupole component has never been clearly observed in the $L_2$ edge. In this work we present a detailed study of the XMCD at the Nd $L_2$ and $L_3$ edges in $Nd_2Fe_{14}B$ as a function of temperature. Our aim is to determine the multipolar nature of the different features in the XMCD spectra by monitoring their temperature dependence through the spin reorientation transition occurring at low temperatures. The occurrence of this magnetic transition in $Nd_2Fe_{14}B$ provides a direct way to verify the existence of quadrupolar transitions to the XMCD spectra. Indeed, one possibility to test the importance of the quadrupolar terms is to measure the dependence of the dichroic signal on the angle $\theta$ between the photon wave vector $\mathbf{k}$ and the magnetization direction. The MCD intensitity depends on $\theta$ as $\cos\theta$ for the $E1$ transition but it is known to depend on $\theta$ in a more complicated way for the $E2$ one. The angular dependence for features associated with dipolar and quadrupolar transitions is given, respectively, by the expressions (Ref. 4)

 © 1998 The American Physical Society

$$\mu_c^{E1}=\frac{6\pi N}{k}(w_{11}-w_{1-1})\cos\,\theta \tag{1a}$$

and

$$\mu_c^{E2}=\frac{10\pi N}{k}[(w_{22}-w_{2-2})\sin^2\theta + (w_{21}-w_{2-1})\cos 2\theta]\cos\,\theta, \tag{1b}$$

where $\mu_c=\mu_c^{E1}+\mu_c^{E2}$. Here $N$ is the number of atoms per unit volume, $w_{lm}$ are the matrix elements of the transitions, and $\theta$ is the angle between the photon wave vector **k** and the local magnetization direction.

The magnetization of $Nd_2Fe_{14}B$ is parallel to the $c$-axis of the tetragonal crystal structure (space group $P4_2/mnm$) at room temperature. Below $T_s\sim 135$ K, there is a second-order spin reorientation transition (SRT) that implies that the magnetization tilts away from the $c$-axis towards the [110] direction at lower temperatures, making an angle $\theta_S(T)$ with the $c$-axis which increases continuously as the temperature decreases and reaches 30.6° at 4.2 K.[7] Therefore, the study of the temperature dependence of the XMCD throughout the SRT transition is equivalent to monitor the angular dependence of the different XMCD features as discussed above.

Nd $L_{2,3}$ XMCD spectra were recorded on a single-crystal $Nd_2Fe_{14}B$ specimen at the European Synchrotron Radiation Facility (ESRF) beamline ID12A, by selecting the second harmonic of the undulator HELIOS II spectrum. The circular polarization rate of the undulator radiation was estimated to be about 90%.[8]

XMCD signals were obtained through the difference of x-ray absorption spectra recorded consecutively either by reversing the helicity of the incident beam or by flipping the magnetic field ($\sim$1 T) generated by a superconducting electromagnet and applied along the beam direction. The spectra were recorded at different fixed temperatures in the fluorescent detection mode. The sample was mounted with the incident plane tilted 45° away from the beam direction, so that both the [001] and [110] directions form a 45° angle, within the orbit plane, with the incident beam. A detailed description of the experimental setup and magnetic characterization of the sample can be found elsewhere.[9] It should be noted that according to our experimental setup, the $\theta$ angle appearing in Eq. (1a) and Eq. (1b) is given by $\theta=45°-\theta_S$.

The spin-dependent absorption coefficient was obtained as the difference of the absorption coefficient $\mu_c=(\mu^- -\mu^+)$ for antiparallel, $\mu^-$, and parallel, $\mu^+$, orientation of the photon helicity and the magnetic field applied to the sample. The spectra were normalized to the averaged absorption coefficient at high energy, $\mu_0$, in order to eliminate the dependence of the absorption on the sample thickness, so that $\mu_c(E)/\mu_0=(\mu^-(E)-\mu^+(E))/\mu_0$ corresponds to the dimensionless spin-dependent absorption coefficient.

The XMCD spectra recorded at temperatures above (250 K) and below (50 K) the spin reorientation transition at both the Nd $L_2$ and $L_3$ edges in the $Nd_2Fe_{14}B$ single crystal are shown in Fig. 1. In both Nd $L_2$ and $L_3$ cases, the main feature of the XMCD spectrum is a positive peak (which we will label $D$) at the absorption threshold that is addressed to the dipolar $E1$ component. The shape and the sign of the main peak in the XMCD signals at the different absorption edges, shown in Fig. 1, are consistent to those previously reported for $R$-Fe intermetallic compounds. Moreover, no modification of the shape or sign of this peak is observed when cooling down through the spin reorientation transition, indicating that no change of the magnetic coupling takes place during the SRT. In a previous work we have demonstrated that the integrated-intensity of the main positive peak of both Nd $L_2$ and $L_3$ XMCD signals reflects the temperature dependence of the projection along the x-ray wave vector of the Nd magnetic moment, $\mu_{Nd}(T)$.[9,10] In other words, they are proportional to $\mu_{Nd}(T)\cos(45°-\theta_{Nd}(T))$, where $\theta_{Nd}(T)$ is the canting angle of $\mu_{Nd}$ in respect to the $c$-axis. The $\theta_{Nd}$ angle has been determined to reach 58° at 4.2 K, giving rise to a noncollinear arrangement of the Nd and Fe moments in the low-temperature magnetic phase.[11]

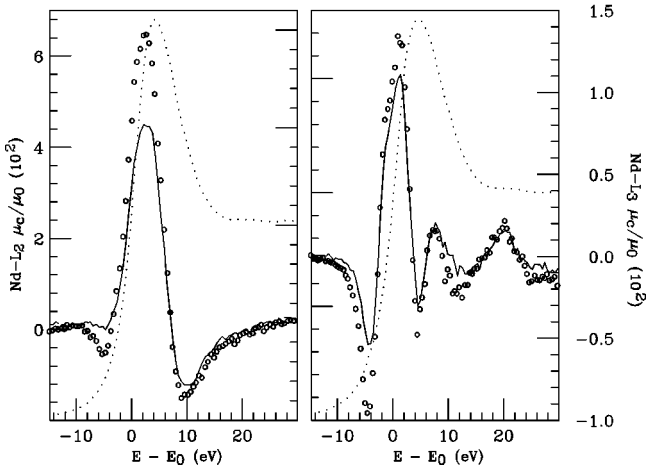


FIG. 1. Left panel. Normalized Nd $L_2$-edge XMCD spectra ($\times 10^2$) recorded at $T=50$ K (○) and $T=250$ K (solid line). The spin averaged absorption recorded $T=250$ K is also shown (dotted line). In the right panel, the same comparison is shown in the case of the Nd $L_3$ edge.

Below the absorption edge the Nd $L_3$-edge XMCD spectra present an intense negative peak (that we refer in the

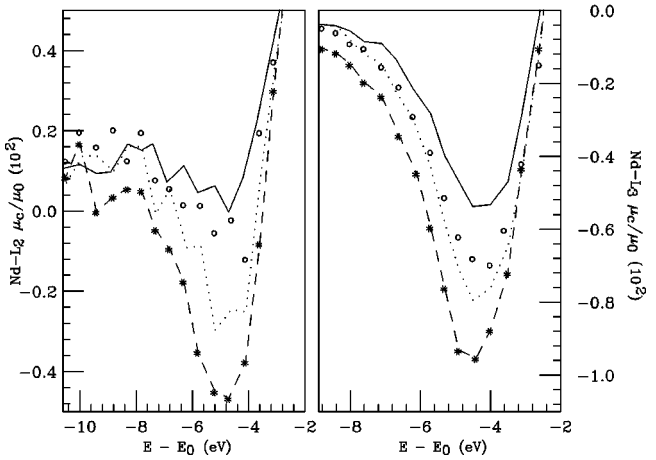


FIG. 2. Temperature dependence of the prominent peaks below the absorption edge in the XMCD spectra recorded at the Nd $L$ edges in $Nd_2Fe_{14}B$: Nd $L_2$ (left panel), and Nd $L_3$ edge (right panel). $T=250$ K (solid line), $T=150$ K (○), $T=130$ K (dotted line), and $T=20$ K (*).

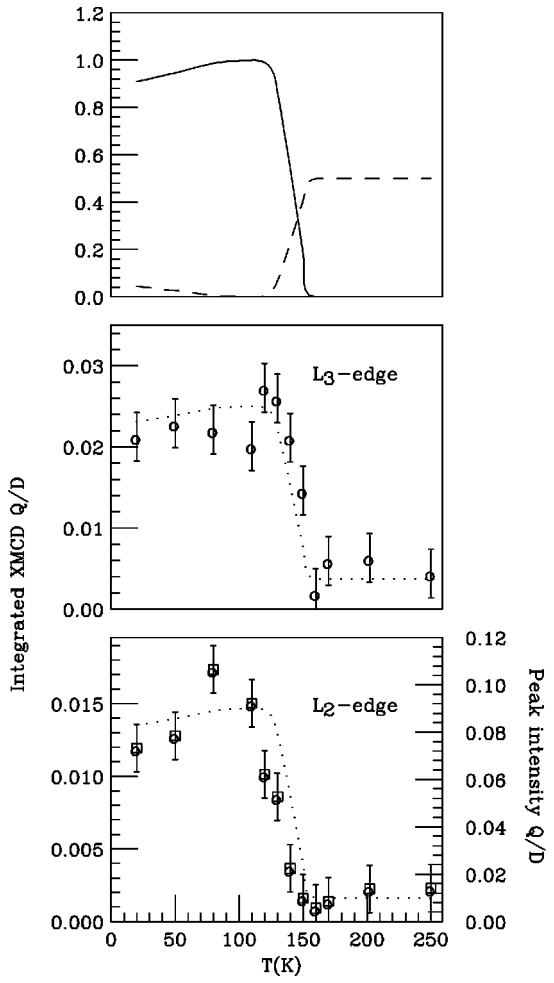


FIG. 3. $Q/D$ temperature dependence of the integrated XMCD $Q$ and $D$ peaks (○) in the Nd $L_2$ (bottom) and $L_3$ edge (middle panel) XMCD spectra. The dotted line corresponds to the simulation of the quadrupolar angular dependence according to $A\sin^2\theta + B\cos 2\theta$. In the case of Nd $L_2$ edge, the ratio of the peak intensity (□) is shown for sake of comparison. In the top panel the two terms of the quadrupolar angular dependence $\cos 2\theta$ (solid line) and $\sin^2\theta$ (dashed) are shown.

following as $Q$), $\sim -4.4$ eV, whose intensity exhibits a huge increase at low temperatures, in contrast to the behavior shown by the $D$ peak. The different modification of the amplitude as a function of temperature is a first sign of its quadrupolar nature, because the temperature dependence of the XMCD is intrinsically linked in $Nd_2Fe_{14}B$ with the dependence of the dichroic signal on the angle $\theta$ between the photon wave vector **k** and the Nd magnetic moment direction. The same trend is observed at the Nd $L_2$-edge XMCD signal. At temperatures above the SRT transition, a very weak negative feature is detected below the prominent positive peak. However, as the temperature is decreased through the SRT, the negative peak, centered at about $-4.7$ eV, is strongly enhanced. The detailed evolution of the negative features below both the Nd $L_2$ and $L_3$ edges is reported in Fig. 2.

The different temperature dependence of the negative and positive main features of the XMCD spectra at both Nd $L_2$ and $L_3$ edges suggest the quadrupolar origin of the negative feature $Q$. In order to verify this assignment, we have studied the temperature dependence of the $Q/D$ intensity ratio.

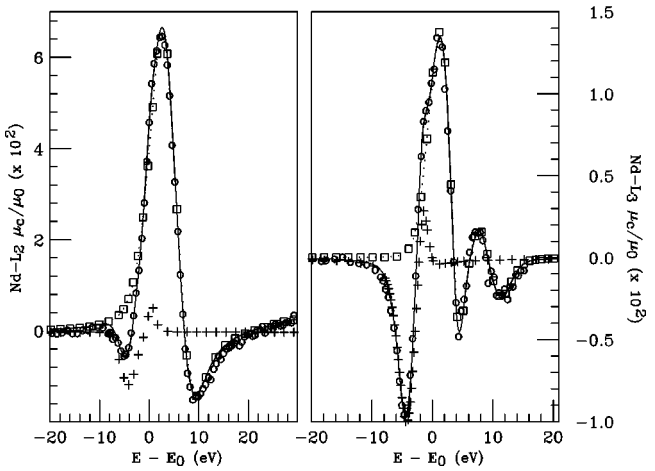


FIG. 4. Deconvolution of the Nd $L_2$ (left) and $L_3$-edge (right) XMCD signals in $Nd_2Fe_{14}B$ recorded at 50 K: (○) experimental data, (□) $E1$-dipolar contribution, (+) $E2$-quadrupolar, (solid line) total $E1+E2$ contribution.

According to expressions Eq. (1a) and Eq. (1b), if both features were of dipolar origin the $Q/D$ ratio is expected to be constant. On the contrary, if the negative feature is of quadrupolar origin, it should be expected that the $Q/D$ ratio presents a temperature dependence departing from a constant value. The experimental temperature dependence of the $Q/D$ ratio for both Nd $L_2$ and $L_3$ is shown in Fig. 3. As clearly shown in the figure, the departure of the dipolarlike behavior is evident. Moreover, if the $Q$ peak is of quadrupolar origin, the $Q/D$ ratio should carry an angular dependence of the type $(w_{22}-w_{2-2})\sin^2\theta+(w_{21}-w_{2-1})\cos 2\theta$, where $\theta=45°-\theta_{Nd}(T)$, and $\theta_{Nd}(T)$ is the angle formed by the Nd magnetic moment and the $c$-axis in the $Nd_2Fe_{14}B$ single crystal. We have fitted the temperature dependence of the $Q/D$ ratio to its angular dependence predicted by Eqs. (1a) and (1b) for a $E2/E1$ ratio, i.e., the linear combination $A\sin^2\theta + B\cos 2\theta$, by using the $\theta_{Nd}(T)$ values obtained from Refs. 9–11. The agreement of the fit to the experimental $Q/D$ ratio is remarkably good for both $L_2$ and $L_3$ edges, supporting our assignment of a quadrupolar origin for the negative feature found in both XMCD spectra. Moreover, our analysis returns that the $(w_{21}-w_{2-1})\cos 2\theta$ component of the quadrupolar transition dominates over $(w_{22}-w_{2-2})\sin^2\theta$, although this last component is also present, as demonstrated for the nonzero value of the $Q/D$ ratio at temperatures above the spin reorientation transition. It is also important to note that this experimental identification of the quadrupolar origin of the features below the absorption edge at both Nd $L_2$ and $L_3$ XMCD spectra in $Nd_2Fe_{14}B$ confirms a recent theoretical prediction about the relative magnitude of the quadrupole contributions, being found that the quadrupole part is always relatively smaller at the $L_2$ edge.[12]

Finally, we present in Fig. 4 the deconvolution of the XMCD spectra at both $L_{2,3}$ edges recorded at 50 K into their dipolar and quadrupolar contributions, taking advantage of a recent RIXS experiment that allowed us to separate and determine the resonance incident energy of the different excitation channels present near the $L_3$ absorption edge.[13] The assumed double feature ''positive-to-negative'' for the spectral shape of the quadrupolar contribution to the dichroic

signal in light rare-earth systems is a direct result of the cited RIXS experiment, in agreement with recent theoretical calculations[14] and the analysis of resonant x-ray magnetic scattering (XRMS) experiments performed on the same sample.[15] The deconvolution has been performed by fitting the dichroic spectra by a combination of pseudovoigt profiles centered at the quadrupolar and main dipolar resonant incident energies determined by RIXS experiments plus some *ad-hoc* included profiles to give account of the higher energy XMCD oscillations. The fit extended over $\approx 80$ eV around the edges. This procedure, performed for the whole set of XMCD spectra, allows us to integrate the dichroic signals in a wider energy range. The $Q/D$ intensity ratio obtained in this way fully confirmed the results previously presented in Fig. 3 by direct integration of the experimental data.

In conclusion, we report an x-ray circular magnetic dichroism (XCMD) experiment performed at the Nd $L_2$ and $L_3$ edges in $Nd_2Fe_{14}B$ as a function of temperature. The intrinsic angular dependence linked to the existing spin reorientation transition occurring at low temperatures allow us to identify the quadrupolar origin of the features below the absorption edges. To the authors' knowledge this is the first experimental observation of a quadrupolar transition at the $L_2$-edge XMCD spectrum of a rare earth. Our results confirm previous theoretical predictions regarding the presence and relative intensity of $E2$ transitions at the $L_{2,3}$ edges of rare earths.[4,12]

This work was partially supported by the INFN-CICYT Agreement and Spanish DGI-CYT MAT96-0448 grants. The experimental work at the European Synchrotron Radiation Facility has been performed with the approval of the ESRF Program Advisory Committee (Proposal HC-543).

[1] B. T. Thole *et al.*, Phys. Rev. Lett. **68**, 1943 (1992); P. Carra *et al.*, *ibid.* **70**, 694 (1993).
[2] P. Carra, Synchrotron Radiation News **5**, 21 (1992); C. T. Chen *et al.*, Phys. Rev. Lett. **75**, 152 (1995).
[3] G. Schütz *et al.*, Z. Phys. B **73**, 67 (1988); P. Fischer *et al.*, Solid State Commun. **76**, 777 (1990); F. Baudelet *et al.*, Europhys. Lett. **13**, 751 (1990); J. Chaboy *et al.*, J. Phys. IV **7**, C2 (1997).
[4] P. Carra and M. Altarelli, Phys. Rev. Lett. **64**, 1286 (1990); P. Carra *et al.*, *ibid.* **66**, 2495 (1991).
[5] M. H. Krisch *et al.*, Phys. Rev. Lett. **74**, 4931 (1995).
[6] J. C. Lang *et al.*, Phys. Rev. Lett. **74**, 4935 (1995).
[7] For a review, see J. F. Herbst, Rev. Mod. Phys. **63**, 819 (1991), and references therein.
[8] J. Goulon *et al.*, Physica B **208&209**, 199 (1995).
[9] D. Givord *et al.*, J. Appl. Phys. **63**, 3713 (1988); J. Chaboy *et al.*, Phys. Rev. B (to be published).
[10] J. Chaboy *et al.*, Europhys. Lett. **28**, 135 (1994).
[11] H. Onoedera *et al.*, J. Magn. Magn. Mater. **68**, 15 (1987).
[12] M. van Veenendaal *et al.*, Phys. Rev. Lett. **78**, 1162 (1997).
[13] F. Bartolomé *et al.*, Phys. Rev. Lett. **79**, 3775 (1997).
[14] M. van Veenendaal and R. Benoist (unpublished).
[15] F. Bartolomé *et al.* (private communication).